Chemical Science

ROYAL SOCIETY OF CHEMISTRY

EDGE ARTICLE

View Article Online
View Journal | View Issue

Check for updates

Cite this: *Chem. Sci.*, 2021, **12**, 5811

All publication charges for this article have been paid for by the Royal Society of Chemistry

A *tellura*-Baeyer–Villiger oxidation: one-step transformation of tellurophene into chiral tellurinate lactone†‡

Shitao Wang, Chaoxian Yan, Wenlong Zhao, Xiaolan Liu, Cheng-Shan Yuan, Hao-Li Zhang and Xiangfeng Shao *

Received 21st January 2021
Accepted 8th March 2021

DOI: 10.1039/d1sc00397f

rsc.li/chemical-science

Baeyer–Villiger (BV) oxidation is a fundamental organic reaction, whereas the hetero-BV oxidation is uncharted. Herein, a *tellura*-BV oxidation is discovered. By oxidizing a tellurophene-embedded and electron-rich polycycle (**1**) with *m*CPBA or Oxone, an oxygen atom is inserted into the Te–C bond of the tellurophene to form tellurinate lactone ***mono*-2**. This reaction proceeds as follows: (i) **1** is oxidized to the tellurophene Te-oxide form (**IM-1**); (ii) **IM-1** undergoes *tellura*-BV oxidation to give ***mono*-2**. Moreover, the hybrid trichalcogenasumanenes **7** and **8** are, respectively, converted to tellurinate lactones ***mono*-9** and ***mono*-10** under the same conditions, indicating that *tellura*-BV oxidation shows high chemoselectivity. Due to the strong secondary bonding interactions between the Te=O groups on tellurinate lactones, ***mono*-2**, ***mono*-9**, and ***mono*-10** are dimerized to form U-shaped polycycles **2**, **9**, and **10**, respectively. Notably, ***mono*-2**, ***mono*-9**, ***mono*-10**, and their dimers show chirality. This work enables one-step transformation of tellurophene into tellurinate lactone and construction of intricate polycycles.

Introduction

The Baeyer–Villiger (BV) oxidation was discovered more than a century ago,[1,2] and great efforts were devoted to making BV oxidation catalytic, along with high chemo-, regio-, and stereoselectivity.[3–7] In BV oxidation, the C–C bond adjacent to the carbonyl is opened and an oxygen atom is inserted to form C–O–C (see Scheme 1a for a typical example). The BV oxidation is an efficient way to transform ketones into esters and/or lactones and is employed to synthesize intricate chemicals.[3–7] A variety of oxidants can be used to perform BV oxidation, such as *meta*-chloroperbenzonic acid (*m*CPBA), H_2O_2, Oxone, and so forth.[8–10] According to the reaction mechanism of BV oxidation, which involves an intermediate known as the Criegee adduct,[11] one may speculate whether it is possible to achieve hetero-BV oxidation. For instance, do organic compounds containing sulfoxide, selenoxide, or telluroxide undergo BV-type oxidation to form the corresponding esters and/or lactones?

Chalcogens (O, S, Se, and Te) have drawn tremendous interest in chemistry and materials science. Tellurium is the heaviest member of this family and shows maverick chemistry.[12–17] The emerging development of tellurium compounds is apparent from their application in catalysis,[18–21] coordination,[22–26] and optoelectronic materials.[27–34] The low Pauling electronegativity and high polarisability of tellurium lead to strong secondary bonding interactions (SBIs) and/or

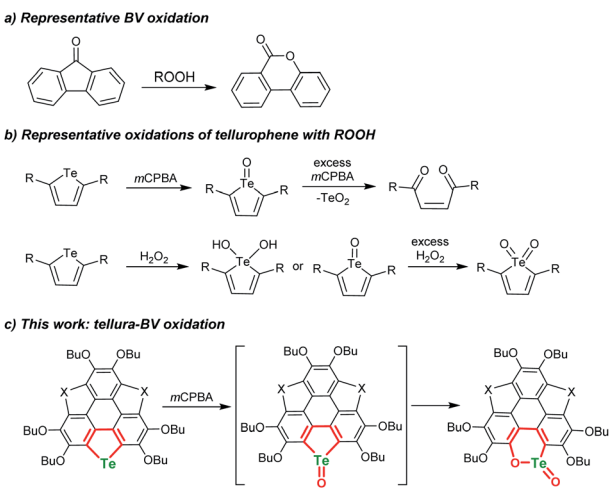

Scheme 1 Schematic illustration of BV oxidation, oxidation of tellurophene by ROOH, and *tellura*-BV oxidation herein.

State Key Laboratory of Applied Organic Chemistry, Lanzhou University, Tianshui Southern Road 222, Lanzhou 730000, China. E-mail: shaoxf@lzu.edu.cn

† Dedicated to Prof. Zhongli Liu on the occasion of his 80th birthday.

‡ Electronic supplementary information (ESI) available: Synthetic procedures, ^{1}H-NMR, ^{13}C-NMR spectra, HRMS, IR, single crystal structure, UV, CD, theoretical calculations and TGA. CCDC 2035868, 2035866, 2035865, 2035863, 2064765 and 2064766. For ESI and crystallographic data in CIF or other electronic format see DOI: 10.1039/d1sc00397f

hypervalent states.[12,35–38] Meanwhile, embedding Te onto the π-scaffolds of organotellurium compounds will narrow the HOMO–LUMO energy gap,[39–42] produce intermolecular Te···X SBIs in the solid state,[43–45] and alter their chemical behavior.[46–52] Recently, Seferos's group performed the oxidation of tellurophenes with peroxides and found that they can be converted to various states including dihydroxy tellurophenes, telluroxides and tellurones (Scheme 1b).[53,54] Further oxidation of tellurophene Te-oxide with *m*CPBA resulted in ring cleavage to form but-2-ene-1,4-dione instead of tellurinate lactone.[53]

In BV oxidation, the migration step is rate-determining in most cases and electron-donating substituents in the migrating group will promote the rearrangement[8–10,55] Herein, with the intention of exploring hetero-BV oxidation, we chose tellurophene-embedded and electron-rich polycycles as substrates. By oxidizing them with *m*CPBA or Oxone, we discovered a *tellura*-BV oxidation (Scheme 1c). To the best of our knowledge, this kind of reaction has never been reported so far. This work enables the one-step conversion of tellurophene into chiral tellurinate lactone. Moreover, this reaction shows excellent chemoselectivity, *i.e.*, only *tellura*-BV oxidation selectively occurs even if telluro-, seleno-, and thiophene moieties coexist in the substrates.

Results and discussion

An electron-rich polycycle **1** containing a tellurophene moiety was prepared from 2,3,6,7,10,11-hexabutoxytriphenylene (**HBT**) *via* the dilithiation and insertion of tellurium in one-pot (see the ESI‡).[56–58] Upon oxidation of **1** by *m*CPBA (2 equiv., condition *a*) in CH_2Cl_2 at room temperature (r.t.), compound **2** was obtained in a yield of 52% (Scheme 2). The yield of **2** remained almost unchanged when excess *m*CPBA was used. On the other hand, compound **2** was harvested with a yield up to 82% by oxidizing **1** with Oxone (2 equiv., condition *b*) in a mixed solvent of THF–deionized water (4 : 1, v/v). It is worth noting that the yield of **2** was distinctly lowered when tap water was used during the oxidation of **1** with Oxone. The reason is that the residual Cl^- in tap water is converted to chlorine in the presence of Oxone,[59,60] and chlorine will react with the tellurophene on **1** to form a hypervalent adduct.[46–49,57]

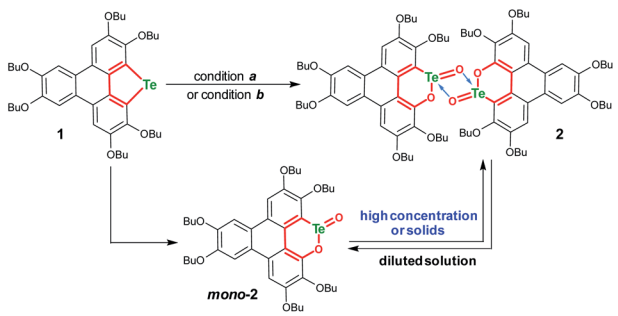

Scheme 2 Transformation of **1** into dimeric tellurinate lactone **2**. Reagents and conditions: (a) *m*CPBA (2 equiv.), CH_2Cl_2, r.t., 4 h, and yield 52%; (b) Oxone (2 equiv.), THF–deionized H_2O (4 : 1, v/v), r.t., 4 h, and yield 82%.

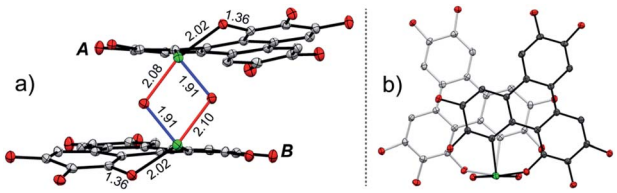

Fig. 1 Crystal structure of **2**, with *n*-Bu groups and hydrogen atoms omitted for clarity. (a) and (b) are, respectively, projected perpendicular and parallel to the "Te_2O_2" four-member ring. The selected bond lengths are shown in units of Å. The C, O, and Te atoms are, respectively, shown in grey, red, and green.

The structure of **2** was also determined through X-ray single crystal structure analysis. Referring to the crystal structure of **2** (Fig. 1), the tellurophene ring on **1** was opened and an oxygen atom was inserted to form six-member rings (**A** and **B** moieties). The bond lengths for the newly formed Te–O and O–C bonds in the **A** and **B** moieties are 2.02(1) and 1.36(1) Å, respectively (Fig. 1a). The **A** and **B** moieties are connected with a "Te_2O_2" four-member ring. The tellurium atoms in the "Te_2O_2" unit take the so-called four-center ten electron (10-E-4) hypervalent state.[12] The "Te_2O_2" four-member ring is nearly perpendicular to the **A** and **B** moieties. As a result, compound **2** adopts a U-shaped conformation (Fig. 1b). According to the molecular structure of compound **2**, this compound is non-centrosymmetric, and therefore it is a chiral molecule. However, a pair of enantiomers coexists in its crystal.

There are two kinds of Te–O bonds in the "Te_2O_2" four-member ring of **2** with bond lengths of 1.91(1) and 2.09(1) Å (Fig. 1a). The former is close to the Te=O bond length (1.89(1) Å) in $PhTeO_2$ (ref. 61) and $(C_6F_5)_2TeO$,[62] and the latter is longer than the Te–O bond (1.97 Å) in $X[(R_2TeO)_nTeR_2]X$.[61,63] It was reported that the Te–X bond (where X is more electronegative than Te) is more polar in Te=X, leading to stronger SBIs.[12] For instance, the telluroxides usually exist as dimers owing to the strong intermolecular O → Te SBIs.[64–67] Therefore, compound **2** can be regarded as a dimer of ***mono*-2** formed through the intermolecular SBIs between the Te=O bonds (Scheme 2). Accordingly, the two kinds of Te–O bonds in "Te_2O_2" can be reasonably assigned to Te=O (1.91(1) Å) and O → Te (2.09(1) Å).

Consistent with the above deduction, we observed the ionic peak of ***mono*-2** ($C_{42}H_{58}O_8Te + H^+$, 821.3257) in the high resolution mass spectrum (HRMS) of **2** as shown in Fig. 2a. This result implies that the dimerization of ***mono*-2** to form **2** would be reversible under certain conditions. In this context, we carried out ^1H NMR spectroscopic investigation of **2** at different concentrations (Fig. 2b). The transformation between ***mono*-2** and **2** occurs indeed. It is found that compound **2** exists in the solution with a concentration higher than 4×10^{-4} mol L^{-1}. As the concentration decreases, ***mono*-2** gradually appears. When the concentration is below 8×10^{-5} mol L^{-1}, compound **2** completely transforms into ***mono*-2**. On the other hand, the single crystals of **2** were harvested by slowly evaporating the solution of ***mono*-2** ($c \leq 8 \times 10^{-5}$ mol L^{-1}). Therefore, ***mono*-2** is

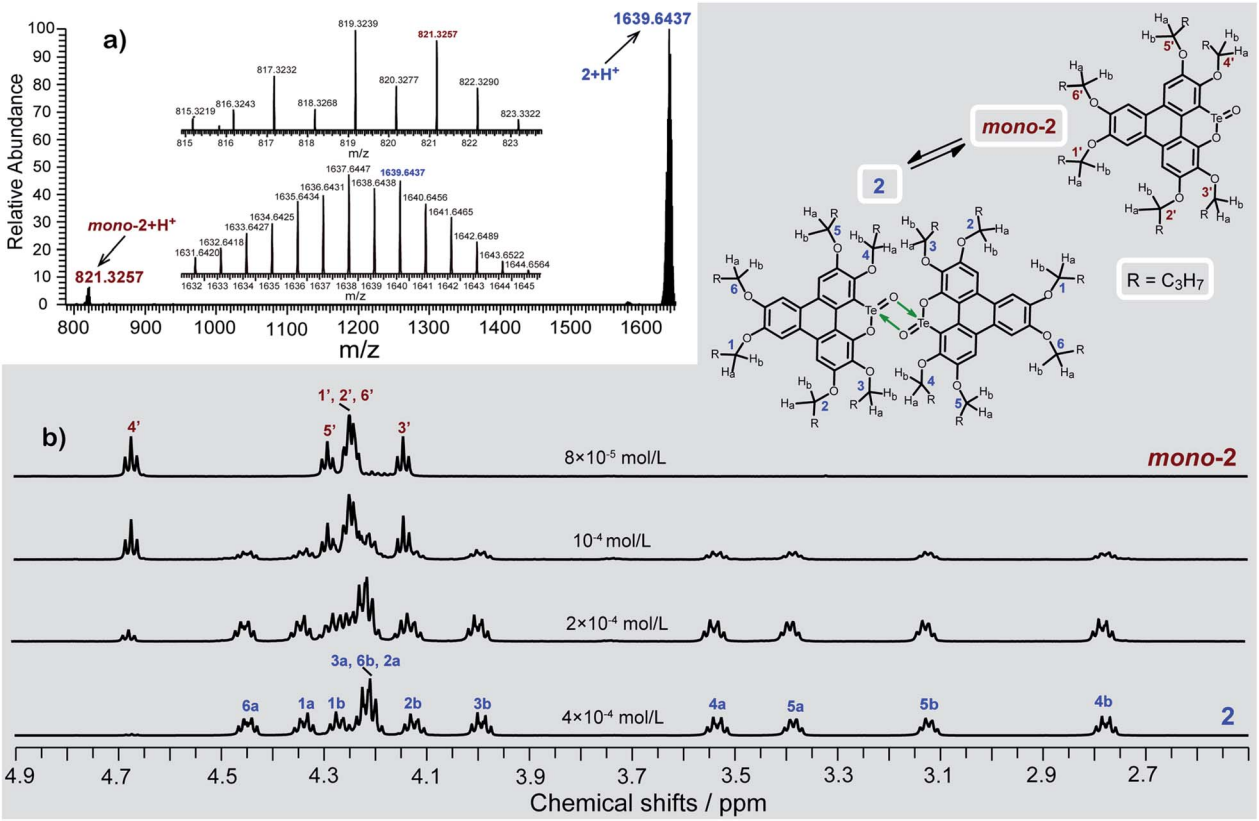

Fig. 2 (a) HRMS spectrum and (b) variable-concentration ^{1}H NMR spectra (*n*-butoxy region) in $CDCl_3$ (600 MHz) of **2**. The protons of **2** (*n*-butoxy region) are assigned with the assistance of two-dimensional NMR spectroscopy (Fig. S2–S6 and Tables S2, S3 in the ESI‡).

the intrinsic product for the oxidation of **1** under condition *a* or *b*.

The product ***mono*-2** possesses a tellurinate lactone moiety, which would have originated from the oxidation of tellurophene Te-oxide. The formation of tellurinate lactone can be rationalized with a *tellura*-BV oxidation mechanism. We have proposed a mechanism for this transformation by employing *m*CPBA as an oxidant (Scheme 3). The tellurophene on **1** is first oxidized by *m*CPBA to afford a tellurophene Te-oxide intermediate **IM-1**.[53] Owing to the highly polarized Te=O bond,[12] the **IM-1** is easily attacked by *m*CPBA to form an intermediate **IM-2**, which resembles the Criegee adduct in BV oxidation. Finally, **IM-2** undergoes a rearrangement to afford ***mono*-2**. Then ***mono*-2** is dimerized in the concentrated solution and/or in the solid state to give **2**. The reaction of **1** with Oxone would also follow the similar procedure. The high yield of **2** under condition *b* can be attributed to the acceleration of the rearrangement step, because the electron-deficient leaving group will facilitate the rearrangement.[3–7]

To gain more insight into the mechanism, an attempt was made to identify the key intermediate **IM-1** along the reaction pathway. It is known that tellurophene can be transformed into its Te-oxide form by oxidation with *m*CPBA.[53] Thus, we

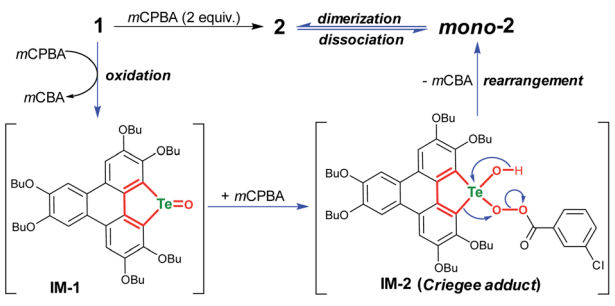

Scheme 3 Proposed mechanism for converting **1** to **2** *via tellura*-BV oxidation.

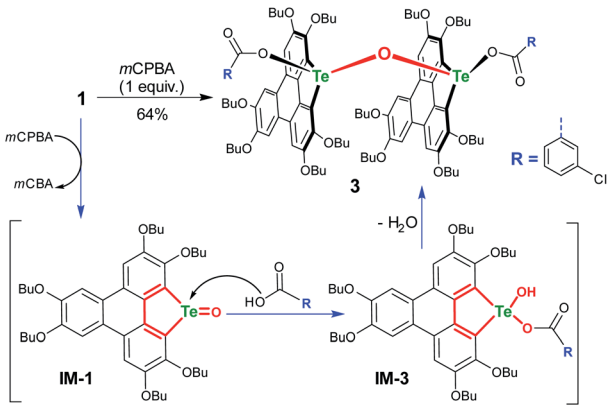

Scheme 4 Oxidation of **1** with *m*CPBA (1 equiv.) in CH_2Cl_2 at r.t.

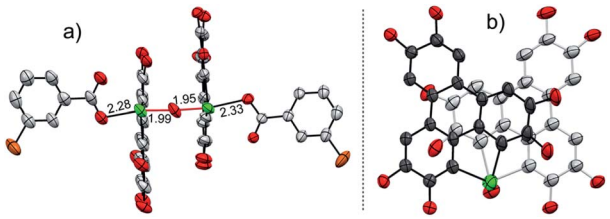

Fig. 3 Crystal structure of **3**, with *n*-Bu groups and hydrogen atoms omitted for clarity. (a) and (b) are, respectively, projected perpendicular and parallel to the **HBT** ring. The *m*CBA moieties are omitted in (b). The Cl atoms are shown in orange.

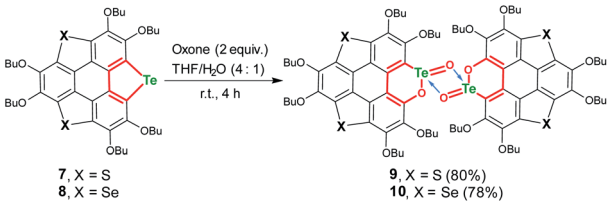

Scheme 6 Conversion of **TCSs 7/8** into dimeric tellurinate lactones **9/10**.

performed the oxidation of compound **1** with 1 equivalent of *m*CPBA (Scheme 4). However, **IM-1** cannot be isolated from the reaction mixture. Instead, compound **3** was obtained and its structure was confirmed by crystallographic analysis (Fig. 3). Because the Te=O bond is prone to attack by nucleophiles,[53] compound **3** would be generated *via* the **IM-1** intermediate as follows: (i) compound **1** is oxidized by *m*CPBA to give **IM-1**, and *m*CPBA is reduced to *meta*-chlorobenzonic acid (*m*CBA); (ii) the **IM-1** is attacked by *m*CBA to form an intermediate **IM-3**; (iii) the dehydration between two **IM-3** molecules affords **3**.[68,69] This means that **IM-1** is indeed formed when **1** is oxidized by *m*CPBA.

Referring to the crystal structure of **3**, the Te–O bonds (2.28–2.33 Å) between *m*CBA ester and Te are much longer than the typical Te–O single bond (1.97 Å),[61] implying that the dissociation of these Te–O bonds would occur to recover **IM-1** under certain conditions. Actually, the HRMS spectrum of **3** shows only the ionic peak of **IM-1** ($C_{42}H_{58}O_7Te + H^+$, 805.3340). We also found that **3** was transformed into **2** when excess *m*CPBA was added. The transformation of **3** into **2** is therefore interpreted as follows: (i) the *m*CBA ester groups on **3** are hydrolyzed under acidic conditions (herein, *m*CPBA), followed by breaking of the Te–O–Te bridge to form **IM-1**; (ii) the **IM-1** undergoes *tellura*-BV oxidation and successive dimerization to afford **2**.

We then studied the electronic effect on *tellura*-BV oxidation. Employing a similar synthetic approach to that of compound **1**, a polycycle containing a tellurophene moiety (compound **4**) was prepared from phenanthrene. In comparison with **1**, compound **4** doesn't possess the electron-rich substituents. As shown in Scheme 5, oxidation of **4** with excess *m*CPBA didn't afford tellurinate lactone **6**, and only **5** was isolated. The formation of **5** is attributed to the transesterification during the purification of crude products *via* column chromatography, where the eluent contains formic acid. Along with previous reports,[53,54] the present result further indicates that electron-donating substituents are essential for *tellura*-BV oxidation.

To further understand *tellura*-BV oxidation, we intend to clarify the chemoselectivity of this reaction. Considering that

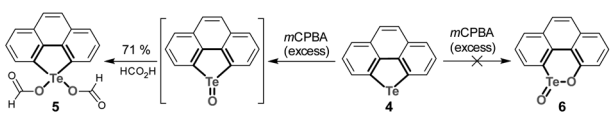

Scheme 5 Oxidation of **4** with excess *m*CPBA in CH_2Cl_2.

electron-donating substituents are required for *tellura*-BV oxidation, trichalcogenasumanenes (**TCSs**) which bear butoxy groups on the flank benzene rings would be suitable substrates. Previously, we achieved the synthesis of such **TCSs**[56–58] and disclosed their chemical reactivities under different conditions.[70–76] Particularly, the oxidative cleavage of flank benzene on trithia- and triselenasumanene was observed by using Oxone as the oxidant.[70] To figure out the chemoselectivity of *tellura*-BV oxidation, we took **TCSs 7** and **8** as substrates, which contain tellurophene and thio-/selenophene moieties (Scheme 6).[58] Upon oxidation by Oxone (2 equiv.), compounds **7** and **8** were, respectively, converted to **9** and **10** which had similar structures to **2**. Notably, the ring-opening of flank benzene and/or oxidation at S/Se atoms of **7/8** was not observed under these conditions. In diluted solution, the "Te_2O_2" four-member rings on **9/10** are dissociated to afford ***mono*-9/*mono*-10**, the same as that of **2**. These results indicate that *tellura*-BV oxidation shows high chemoselectivity, since the chemical reactivities of hybrid **TCSs** are dominated by heavier chalcogenium, as we have concluded previously.[58]

The structures of **9** and **10** were also determined by X-ray single crystal structure analyses. The crystal structures of **9** and **10** show the same features, and Fig. 4 depicts the crystal structure of **10** as a representative example. The molecular

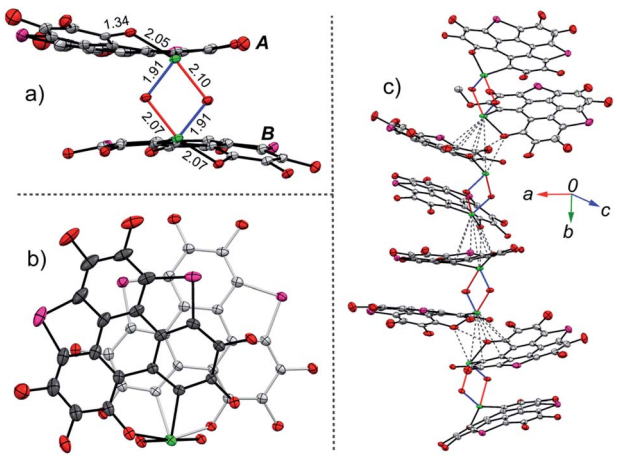

Fig. 4 Crystal structure of **10**, with *n*-Bu groups and hydrogen atoms omitted for clarity: (a) and (b) are molecular structures, respectively, projected perpendicular and parallel to the "Te_2O_2" four-member ring; (c) packing motif with intermolecular contacts shown in grey dashed lines. The Se atoms are shown in pink.

structure of **10** is reminiscent of that of **2**. Two ***mono*-10** are dimerized *via* a "Te_2O_2" four-member ring to form a non-centrosymmetric U-shaped structure. The tellurium atoms on the "Te_2O_2" four-member ring take the "10-E-4" hypervalent state (Fig. 4a). Two kinds of Te–O bonds in "Te_2O_2" are observed with bond lengths of 1.91(1) and 2.07(2) Å, respectively, assigned to Te=O and O → Te. Compound **10** forms helical arrays in the crystal with various intermolecular atomic contacts between neighboring molecules (Fig. 4c), *i.e.*, Te···C (3.44–3.70 Å), Te···O (2.95–3.33 Å), Te···Te (4.06–4.09 Å), and O···O (2.85–3.02 Å). While **10** is a chiral molecule, a pair of enantiomers coexists in its crystal.

It is worth noting that **2**, **9**, and **10** show good thermal stability at a decomposition temperature higher than 200 °C (Fig. S1 and Table S1 in the ESI‡). **2**, **9**, and **10** are solvable in organic solvents such as CH_2Cl_2, $CHCl_3$, toluene, and THF, whereas they show poor solubility in methanol.

We elucidated the influence on electronic states by converting tellurophene into tellurinate lactone and its dimerized form. Herein, we take **8**, ***mono*-10**, and **10** as representative examples, and those for the **1** and **7** series show similar phenomena. Theoretical studies reveal that the HOMO energy levels remain almost unchanged for **8**, ***mono*-10**, and **10**. The LUMO energy levels of ***mono*-10** and **10** are the same, and both are clearly lower than that of **8** (Fig. 5a). This is caused by the electron-withdrawing unit (Te=O) in ***mono*-10** and **10**. Consequently, the HOMO–LUMO energy gaps (E_g) of ***mono*-10** (E_g = 3.75 eV) and **10** (E_g = 3.78 eV) are narrower than that of **8** (E_g = 4.19 eV). Consistent with the theoretical study, the UV-Vis absorption spectra in CH_2Cl_2 for ***mono*-10** ($c = 1 \times 10^{-5}$ mol L^{-1}) and **10** ($c = 5 \times 10^{-4}$ mol L^{-1}) are almost identical (Fig. 5b). The compounds ***mono*-10** and **10** exhibit broad absorption bands at 382–440 nm originating from the HOMO–LUMO transition, which is red-shifted compared to that of **8** (368–414 nm). The compounds ***mono*-10** and **10** are non-emissive at r.t., but they show emissions at 77 K (Fig. 5c), ascribable to phosphorescence. The emission of **10** is clearly red-shifted compared to that of ***mono*-10**, which would be due to the excimer emission since the two π-frameworks of **10** are arranged face-to-face (see Fig. 4b). Similar phenomena are also observed for **2** and **9** (Fig. S26 and S27‡).

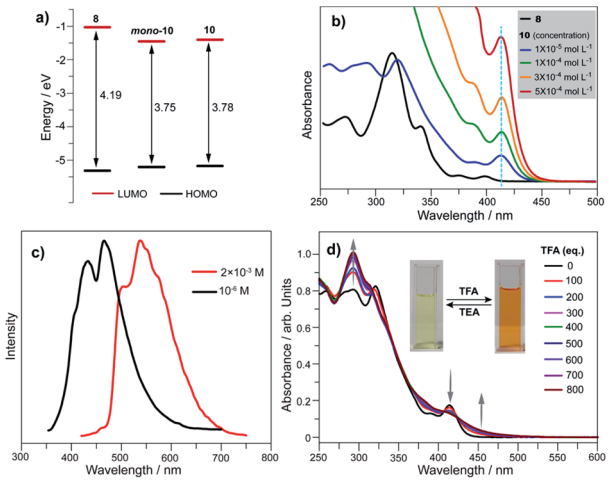

Fig. 5 (a) Calculated energy levels for **8**, ***mono*-10**, and **10**; (b) variable-concentration UV-Vis absorption spectra of **10** in CH_2Cl_2, along with those of **8** ($c = 1 \times 10^{-5}$ mol L^{-1}) for comparison. The cyan dashed line is a guide to the eye for the absorption maximum at long wavelength band. (c) The emission spectra of ***mono*-10** ($c = 1 \times 10^{-6}$ mol L^{-1}) and **10** ($c = 2 \times 10^{-3}$ mol L^{-1}) in THF at 77 K; (d) UV-Vis absorption spectra of **10** in CH_2Cl_2 upon titration with TFA.

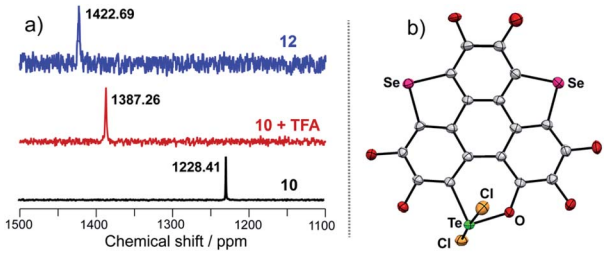

Fig. 6 (a) ^{125}Te NMR of **10**, **12**, and **10** + **TFA** measured in $CDCl_3$, where chemical shifts are recorded using ^{125}Te NMR of diphenyl ditelluride (δ = 420 ppm) as an external reference; (b) crystal structure of **12** with *n*-Bu groups omitted.

Referring to Fig. 5d, the UV-Vis absorption of **10** is distinctly changed upon adding trifluoroacetic acid (TFA). Acidification of **10** also leads to a clear down-field shift of ^{125}Te NMR (Fig. 6a). On the other hand, the original absorption bands and ^{1}H NMR spectra of **10** will be restored when the acidified solution of **10** is neutralized by triethylamine (TEA) as shown in Fig. S25.‡ Thus, it is a reversible process and a proposed mechanism is shown in Fig. S25.‡ Variations in absorption spectra and ^{1}H NMR of **10** are also observed in the presence of HCl (3 N, aqueous). However, the original spectra of **10** are not recovered by neutralization. **10** was quantitatively converted into a new product when it was reacted with HCl (3 N, aqueous). Single crystal structure analysis reveals that the tellurinate lactone moiety of **10** is destroyed and two Cl atoms are attached onto the Te atom to give compound **12** (Fig. 6b). The mechanism for the formation of **12** is shown in Scheme 7.

2, **9**, and **10** possess chirality, whereas they are obtained as enantiomers. We separated the enantiomers of **2**, **9**, and **10** *via* chiral HPLC on a Daicel CHIRALPAK IF (IF00CE-SL018) column (eluent: hexane/CH_2Cl_2 = 50/50). Fig. 7a shows the chiral

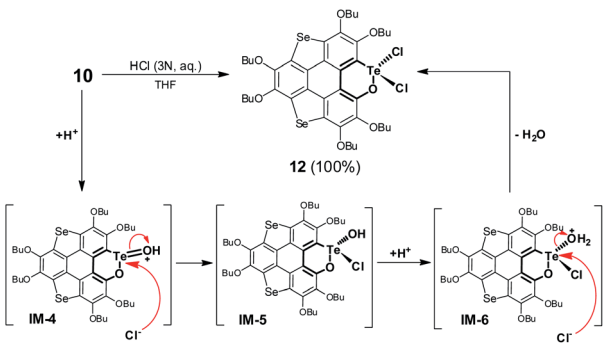

Scheme 7 Transformation of **10** into **12** upon reaction with aqueous HCl.

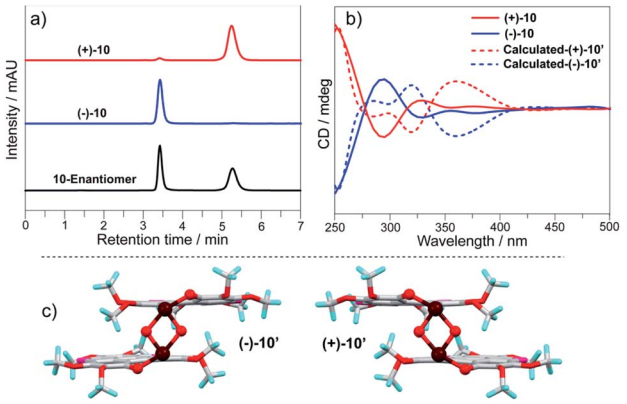

Fig. 7 (a) Chiral chromatograms of **10**; (b) CD spectra of (+)-**10**/(−)-**10** in CH_2Cl_2 ($c = 6 \times 10^{-4}$ mol L^{-1}) along with the simulated ones; (c) molecular structures of (+)-**10′** and (−)-**10′**.

chromatogram of **10** as a typical example. Two fractions of **10** have retention times of 3.4 min and 5.3 min, and are isolated with >93% ee. Circular dichroism (CD) spectra of the two fractions show a mirror symmetry (Fig. 7b), indicating that they have opposite chirality. According to the positive and negative Cotton effects at 378 nm, the two fractions are denoted as (+)-**10** and (−)-**10**. Based on the molecular structure of **10** in a single crystal, we performed CD spectra simulation *via* TD-DFT calculation at the TD-PBE0/Def2-SVP level, where the butyl groups on (+)-**10** and (−)-**10** were replaced with methyl groups to give (+)-**10′** and (−)-**10′**. The simulated CD spectra of (+)-**10′** and (−)-**10′** are in good agreement with the experimental results, and give the structure of each isomer as shown in Fig. 7c.

Conclusions

In summary, we have discovered a *tellura*-BV oxidation which enables the one-step transformation of tellurophene into the chiral tellurinate lactone. Owing to the strong SBIs between Te═O groups, the resulting tellurinate lactone is dimerized *via* the formation of a hypervalent "Te_2O_2" four-member ring in the solid state. This reaction shows good chemoselectivity, *i.e.*, *tellura*-BV oxidation selectively occurs when the telluro-, seleno-, and thiophene moieties coexist in the substrates. It was also found that electron-donating substituents are essential for *tellura*-BV oxidation. Employing *tellura*-BV oxidation as a vital step, the hybrid trichalcogenasumanenes are transformed into the U-shaped polycycles. Further investigation will be directed to the development of stereoselective *tellura*-BV oxidation as well as the asymmetric synthesis and application of the U-shaped polycycles. Such work is ongoing in our laboratory.

Author contributions

S. W. conducted the synthesis, crystal structure analysis, and most of the measurements. C. Y. carried out the theoretical calculation. W. Z. supported the synthesis. X. L. contributed to the ^{125}Te NMR measurement. C.-S. Y. contributed to the analysis of NMR spectra (including 2D NMR). H.-L. Z. contributed to the analysis and discussion on optical spectra. X. S. conceived the ideas and designed the project. S. W. and X. S. wrote the paper. All authors approved the final version of the manuscript.

Conflicts of interest

There is no conflict of interest to report.

Acknowledgements

The authors acknowledge the grant from the National Natural Science Foundation of China (21871119, 21522203) and the National Key R&D Program of China (2017YFA0204903). We greatly appreciate Mr Fengming Qi at SKLAOC for the measurement of ^{125}Te NMR.

Notes and references

1 A. Baeyer and V. Villiger, *Ber. Dtsch. Chem. Ges.*, 1899, **32**, 3625.
2 A. Baeyer and V. Villiger, *Ber. Dtsch. Chem. Ges.*, 1900, **33**, 858.
3 G. R. Krow, in *Organic Reaction: The Baeyer-Villiger Oxidation of Ketones and Aldehydes*, ed. L. A. Paquette, John Wiley & Sons, Inc., 1993, vol. 43.
4 M. Renz and B. Meunier, *Eur. J. Org. Chem.*, 1999, **1999**, 737.
5 G. J. Brink, I. W. C. E. Arends and R. A. Sheldon, *Chem. Rev.*, 2004, **104**, 4105.
6 L. Zhou, L. Lin, X. Liu, and X. Feng, in *Molecular Rearrangements in Organic Synthesis: Baeyer-Villiger Oxidation/Rearrangement in Organic Synthesis*, ed. C. M. Christian, 1st edn, John Wiley & Sons, Inc., 2016, vol. 2.
7 G. Strukul, *Angew. Chem., Int. Ed.*, 1998, **37**, 1198.
8 A. Berkessel, M. R. M. Andreae, H. Schmickler and J. Lex, *Angew. Chem., Int. Ed.*, 2002, **41**, 4481.
9 S.-I. Murahashi, S. Ono and Y. Imada, *Angew. Chem., Int. Ed.*, 2002, **41**, 2366.
10 M. Uyanik, D. Nakashima and K. Ishihara, *Angew. Chem., Int. Ed.*, 2012, **51**, 9093.
11 R. Criegee, *Justus Liebigs Ann. Chem.*, 1948, **560**, 127.
12 T. Chivers and R. S. Laitinen, *Chem. Soc. Rev.*, 2015, **44**, 1725.
13 G. C. Hoover and D. S. Seferos, *Chem. Sci.*, 2019, **10**, 9182.
14 A. Nordheider, J. D. Woollins and T. Chivers, *Chem. Rev.*, 2015, **115**, 10378.
15 L. C. Roof and J. W. Kolis, *Chem. Rev.*, 1993, **93**, 1037.
16 Z. He, Y. Yang, J. W. Liu and S. H. Yu, *Chem. Soc. Rev.*, 2017, **46**, 2732.
17 T. G. Chasteen and R. Bentley, *Chem. Rev.*, 2003, **103**, 1.
18 Z. Dong, X. Li, K. Liang, S. Mao, X. Huang, B. Yang, J. Xu, J. Liu, G. Luo and J. Shen, *J. Org. Chem.*, 2007, **72**, 606.
19 Z. Z. Huang and Y. Tang, *J. Org. Chem.*, 2002, **67**, 5320.
20 I. D. Rettig, J. Van, J. B. Brauer, W. Luo and T. M. McCormick, *Dalton Trans.*, 2019, **48**, 5665.
21 M. Oba, M. Endo, K. Nishiyama, A. Ouchi and W. Ando, *Chem. Commun.*, 2004, 1672.
22 A. Rahaman, G. C. Lisensky, D. A. Tocher, M. G. Richmond, G. Hogarth and E. Nordlander, *J. Organomet. Chem.*, 2018, **867**, 381.

23 A. K. Singh and S. Sharma, *Coord. Chem. Rev.*, 2000, **209**, 49.
24 V. K. Jain and R. S. Chauhan, *Coord. Chem. Rev.*, 2016, **306**, 270.
25 S. Wang, C. Yan, J. Shang, W. Wang, C. Yuan, H.-L. Zhang and X. Shao, *Angew. Chem., Int. Ed.*, 2019, **58**, 3819.
26 I. D. Sadekov, A. A. Maksimenko, A. G. Maslakov and V. I. Minkin, *J. Organomet. Chem.*, 1990, **391**, 179.
27 M. Kaur, D. S. Yang, K. Choi, M. J. Cho and D. H. Choi, *Dyes Pigm.*, 2014, **100**, 118.
28 A. A. Soares-Paulino, L. Giroldo, G. Celante, E. Oliveira, S. M. Santos, R. F. Mendes, F. A. Almeida Paz, A. M. Fioroto, P. V. Oliveira, S. H. P. Serrano, C. Lodeiro and A. A. DosSantos, *Dyes Pigm.*, 2019, **160**, 208.
29 T. Chatterjee, V. S. Shetti, R. Sharma and M. Ravikanth, *Chem. Rev.*, 2017, **117**, 3254.
30 P. F. Li, T. B. Schon and D. S. Seferos, *Angew. Chem., Int. Ed.*, 2015, **54**, 9361.
31 G. Li, L. Xu, W. Zhang, K. Zhou, Y. Ding, F. Liu, X. He and G. He, *Angew. Chem., Int. Ed.*, 2018, **57**, 4897.
32 L. Yang, W. Gu, L. Lv, Y. Chen, Y. Yang, P. Ye, J. Wu, L. Hong, A. Peng and H. Huang, *Angew. Chem., Int. Ed.*, 2018, **57**, 1096.
33 G. Li, B. Zhang, J. Wang, H. Zhao, W. Ma, L. Xu, W. Zhang, K. Zhou, Y. Du and G. He, *Angew. Chem., Int. Ed.*, 2019, **58**, 8468.
34 E. I. Carrera and D. S. Seferos, *Macromolecules*, 2015, **48**, 297.
35 A. J. Mukherjee, S. S. Zade, H. B. Singh and R. B. Sunoj, *Chem. Rev.*, 2010, **110**, 4357.
36 N. W. Alcock and W. D. Harrison, *J. Chem. Soc., Dalton Trans.*, 1982, 1421.
37 J. Beckmann, D. Dakternieks, A. Duthie, N. A. Lewcenko and C. Mitchell, *Angew. Chem., Int. Ed.*, 2004, **43**, 6683.
38 R. Gleiter, G. Haberhauer, D. B. Werz, F. Rominger and C. Bleiholder, *Chem. Rev.*, 2018, **118**, 2010.
39 A. Aprile, K. J. Iversen, D. J. D. Wilson and J. L. Dutton, *Inorg. Chem.*, 2015, **54**, 4934.
40 R. S. Ashraf, I. Meager, M. Nikolka, M. Kirkus, M. Planells, B. C. Schroeder, S. Holliday, M. Hurhangee, C. B. Nielsen, H. Sirringhaus and I. McCulloch, *J. Am. Chem. Soc.*, 2015, **137**, 1314.
41 A. Muranaka, S. Yasuike, C. Y. Liu, J. Kurita, N. Kakusawa, T. Tsuchiya, M. Okuda, N. Kobayashi, Y. Matsumoto, K. Yoshida, D. Hashizume and M. Uchiyama, *J. Phys. Chem. A*, 2009, **113**, 464.
42 M. Planells, B. C. Schroeder and I. McCulloch, *Macromolecules*, 2014, **47**, 5889.
43 M. Bendikov, F. Wudl and D. F. Perepichka, *Chem. Rev.*, 2004, **104**, 4891.
44 R. D. McCullough, G. B. Kok, K. A. Lerstrup and D. O. Cowan, *J. Am. Chem. Soc.*, 1987, **109**, 4115.
45 A. Patra, Y. H. Wijsboom, G. Leitus and M. Bendikov, *Org. Lett.*, 2009, **11**, 1487.
46 E. I. Carrera, A. E. Lanterna, A. J. Lough, J. C. Scaiano and D. S. Seferos, *J. Am. Chem. Soc.*, 2016, **138**, 2678.
47 E. I. Carrera and D. S. Seferos, *Dalton Trans.*, 2015, **44**, 2092.
48 T. M. McCormick, A. A. Jahnke, A. J. Lough and D. S. Seferos, *J. Am. Chem. Soc.*, 2012, **134**, 3542.
49 E. I. Carrera, T. M. McCormick, M. J. Kapp, A. J. Lough and D. S. Seferos, *Inorg. Chem.*, 2013, **52**, 13779.
50 A. Alka, V. S. Shetti and M. Ravikanth, *Dalton Trans.*, 2019, **48**, 4444.
51 L. Latos-Grażyński, E. Pacholska, P. J. Chmielewski, M. M. Olmstead and A. L. Balch, *Angew. Chem., Int. Ed.*, 1995, **34**, 2252.
52 M. Abe, M. R. Detty, O. O. Gerlits and D. K. Sukumaran, *Organometallics*, 2004, **23**, 4513.
53 E. I. Carrera and D. S. Seferos, *Organometallics*, 2017, **36**, 2612.
54 T. M. McCormick, E. I. Carrera, T. B. Schon and D. S. Seferos, *Chem. Commun.*, 2013, **49**, 11182.
55 J. A. Berson and S. Suzuki, *J. Am. Chem. Soc.*, 1959, **81**, 4088.
56 X. Li, Y. Zhu, J. Shao, B. Wang, S. Zhang, Y. Shao, X. Jin, X. Yao, R. Fang and X. Shao, *Angew. Chem., Int. Ed.*, 2014, **53**, 535.
57 S. Wang, X. Li, X. Hou, Y. Sun and X. Shao, *Chem. Commun.*, 2016, **52**, 14486.
58 S. Wang, J. Shang, C. Yan, W. Wang, C. Yuan, H.-L. Zhang and X. Shao, *Org. Chem. Front.*, 2019, **6**, 263.
59 G. Zhao, L. Liang, C. H. E. Wen and R. Tong, *Org. Lett.*, 2019, **21**, 315.
60 J. Ren and R. Tong, *Org. Biomol. Chem.*, 2013, **11**, 4312.
61 N. W. Alcock and W. D. Harrison, *J. Chem. Soc., Dalton Trans.*, 1982, 709.
62 D. Naumann, W. Tyrra, R. Herrmann, I. Pantenburg and M. S. Wickleder, *Z. Anorg. Allg. Chem.*, 2002, **628**, 833.
63 J. Beckmann, D. Dakternieks, A. Duthie, F. Ribot, M. Schürmann and N. A. Lewcenko, *Organometallics*, 2003, **22**, 3257.
64 K. Srivastava, A. Panda, S. Sharma and H. B. Singh, *J. Organomet. Chem.*, 2018, **861**, 174.
65 A. Gupta, R. Deka, A. Sarkar, H. B. Singh and R. J. Butcher, *Dalton Trans.*, 2019, **48**, 10979.
66 J. Beckmann, J. Bolsinger, P. Finke and M. Hesse, *Angew. Chem., Int. Ed.*, 2010, **49**, 8030.
67 J. Beckmann, P. Finke, M. Hesse and B. Wettig, *Angew. Chem., Int. Ed.*, 2008, **47**, 9982.
68 P. Singh, A. K. S. Chauhan, R. J. Butcher and A. Duthie, *Polyhedron*, 2013, **62**, 227.
69 P. Thavornyutikarn and W. R. McWhinnie, *J. Organomet. Chem.*, 1973, **50**, 135.
70 X. Li, Y. Zhu, J. Shao, L. Chen, S. Zhao, B. Wang, S. Zhang, Y. Shao, H.-L. Zhang and X. Shao, *Angew. Chem., Int. Ed.*, 2015, **54**, 267.
71 X. Hou, Y. Zhu, Y. Qin, L. Chen, X. Li, H.-L. Zhang, W. Xu, D. Zhu and X. Shao, *Chem. Commun.*, 2017, **53**, 1546.
72 Y. Sun, X. Li, C. Sun, H. Shen, X. Hou, D. Lin, H.-L. Zhang, C. A. Di, D. Zhu and X. Shao, *Angew. Chem., Int. Ed.*, 2017, **56**, 13470.
73 X. Hou, J. Sun, Z. Liu, C. Yan, W. Song, H.-L. Zhang, S. Zhou and X. Shao, *Chem. Commun.*, 2018, **54**, 10981.
74 X. Hou, Y. Sun, L. Liu, S. Wang, R. Geng and X. Shao, *Chin. Chem. Lett.*, 2016, **27**, 1166.
75 D. Li and X. Shao, *Synlett*, 2020, **31**, 1050.
76 W. Wang and X. Shao, *Org. Biomol. Chem.*, 2021, **19**, 101.